Clinical Neurophysiology 130 (2019) 388–395

Contents lists available at ScienceDirect

Clinical Neurophysiology

journal homepage: www.elsevier.com/locate/clinph

Three-dimensional amplitude characteristics of masseter motor units and representativeness of extracted motor unit samples

Bernd Georg Lapatki [a,*], Ulrike Eiglsperger [a], Hans Jürgen Schindler [b], Johanna Radeke [a], Ales Holobar [c], Johannes Petrus van Dijk [a,d]

[a] Department of Orthodontics, University of Ulm, Albert-Einstein-Allee 11, 89081 Ulm, Germany
[b] Department of Prosthodontics, University of Würzburg, Josef-Schneider-Strasse 2, 97080 Würzburg, Germany
[c] Faculty of Electrical Engineering and Computer Science, University of Maribor, Smetanova Ulica 17, 2000 Maribor, Slovenia
[d] Department of Clinical Physics, Kempenhaeghe Epilepsy and Sleep Center, Sterkselseweg 65, 5591 VE Heeze, the Netherlands

ARTICLE INFO

Article history:
Accepted 9 December 2018
Available online 19 January 2019

Keywords:
Masseter
Electromyography
High-density surface EMG
Scanning EMG
Motor unit
Temporomandibular disorder

HIGHLIGHTS

- High-density surface electromyography (HDsEMG) detects small and large motor units (MUs) located in the outer 70% of the masseter's cross-section.
- HDsEMG detects MUs from the entire muscle surface in one measurement.
- From a 3D point of view, HDsEMG detects the most representative MU sample.

ABSTRACT

Objective: This study aimed to characterize amplitude topographies for masseter motor units (MUs) three-dimensionally, and to assess whether high-density surface electromyography (HDsEMG) is able to detect MU samples that represent the masseter's entire MU pool.
Methods: Ten healthy adult volunteers participated in the study, which combined three EMG techniques. A HDsEMG grid covering the entire masseter, and intramuscular fine-wire electrodes were used to obtain two independent MU samples for comparison. The MUs' amplitude profiles in the dimension of muscle depth were determined using scanning EMG. All data were recorded simultaneously during a low, constant contraction level controlled by 3D force feedback.
Results: The median medio-lateral diameter of 4.4 mm (range: 1.2–7.9 mm) for MUs detected by HDsEMG did not differ significantly (Mann-Whitney-U test, $p = 0.805$) from that of 3.9 mm (0.6–8.6 mm) for MUs detected by fine-wire EMG. For individual subjects, the medio-lateral diameters of all HDsEMG-detected MUs spanned 70.5% (19.2–75.1%) of the masseter's thickness.
Conclusions: HDsEMG is able to examine small and large MUs from a great masseter proportion in one single measurement.
Significance: Clinical application of HDsEMG might contribute to a better understanding of neuromuscular adaptations in patients with temporomandibular disorders (TMD) and could allow for monitoring treatment effects.

1. Introduction

Painful temporomandibular disorders (TMDs) comprise a heterogeneous array of myogenous or arthrogenous disorders of the masticatory system. According to epidemiologic studies, the most common diagnosis for TMD patients is myofascial pain (List and Dworkin, 1996; Manfredini et al., 2011). Alteration of motor unit (MU) recruitment is hypothesized to be a neural reaction to the pain (Falla et al., 2010; Minami et al., 2013). Knowledge of

Abbreviations: TMD, temporomandibular disorder; MU, motor unit; HDsEMG, high-density surface electromyography; PNR, pulse-to-noise ratio; MUAP, motor unit action potential.

* Corresponding author.
E-mail address: bernd.lapatki@uni-ulm.de (B.G. Lapatki).

https://doi.org/10.1016/j.clinph.2018.12.008
1388-2457/

recruitment changes or strategies of the masticatory motor system is largely based on conventional surface EMG (Türp et al., 2002; Falla et al., 2007). Signals recorded with this technique contain the interference from many active MUs. Studies of the behavior of individual MUs are needed for a deeper understanding of the pathophysiologic mechanisms of myofascial pain. Intramuscular EMG, the gold standard method for detailed MU analysis, is not considered a realistic option for clinical application because the invasive measurements it takes could further compromise the already painful muscle. Moreover, needle or fine-wire electrode recordings are rather selective; i.e., they focus on quite small regions of the muscle investigated. Therefore, measurement reproducibility is compromised, and the representativeness of the extracted local MU sample for the muscle's entire MU pool is questionable. Hence, an alternative non-invasive electrophysiological method is needed that can be used to evaluate current pathophysiologic theories on muscle pain at a MU level and optimize therapeutic interventions for TMD patients.

High-density surface electromyography (HDsEMG) uses a large number of small electrode contacts on the skin surface to record spatial and temporal differences of MU action potentials (Blok et al., 2002; Merletti et al., 2009). By combining this method with advanced signal-processing techniques, it is possible to study the behavior of several active individual MUs simultaneously (Holobar and Zazula, 2007; Holobar et al., 2009). Although decomposition of HDsEMG signals has proven highly accurate for a large number of muscles (Holobar et al., 2010, 2014), no studies have assessed the representativeness of the entire MU pool obtained by this approach for a particular muscle.

This study aims to determine spatial characteristics for decomposed individual MUs of the masseter in three dimensions, i.e. on the skin surface and in the muscle depth. The latter will indicate the depth at which individual MUs can be examined in the masseter using HDsEMG. Moreover, by comparing surface amplitude topographies of MU samples recorded by HDsEMG and intramuscular fine-wire EMG, we investigated the hypothesis that HDsEMG records a more representative MU sample from the masseter than fine-wire EMG does. High representativeness is crucial for the application of this electrophysiological method as a non-invasive tool for MU analysis in TMD pain studies.

2. Methods

2.1. Subjects

Ten healthy adult volunteers (four women, six men) with a mean age of 25 years (range: 23–28) participated in this study. All subjects were naturally dentate and had no pain or dysfunction as assessed by means of the Research Diagnostic Criteria for TMD (Dworkin and LeResche, 1992), and no signs of neuromuscular diseases. The study was approved by the local ethics committee of the University of Heidelberg (no. S2013/2008), and all subjects gave their written informed consent prior to the measurements.

2.2. Experimental design

We combined three EMG acquisition techniques (Fig. 1). HDsEMG and intramuscular fine-wire EMG were recorded and independently decomposed to obtain the firing patterns for two comparative MU samples from the masseter. The HDsEMG also provided topographical information about the MUs' amplitude territories on the skin surface. Scanning EMG allowed the MUs' amplitude profiles in the dimension of muscle depth to be determined. To maintain constant contraction and direction—an essential experimental prerequisite—we provided visual 3D force feedback via a PC monitor. All EMG and force data were recorded simultaneously during two separate EMG scans performed at different positions close to the muscle belly.

A data example with indicated firing times of one specific MU in the HDsEMG and fine-wire interference EMG, corresponding HDsEMG and intramuscular EMG MUAP templates and EMG scans is given in Supplementary Fig. S1.

2.2.1. HDsEMG

The HDsEMG electrode grid was positioned in a standardized way to cover the entire right masseter muscle (Fig. 1A). It consisted of 256 regularly arranged silver chloride contacts 1 mm in diameter (Fig. 1C). A previously developed skin attachment procedure (Lapatki et al., 2004) ensured firm electrode grid fixation and low electrode-to-skin impedances, leading to high signal quality.

2.2.2. Intramuscular fine-wire EMG

Prior to each EMG scan we used dental needles (diameter: 0.4 mm, length: 42 mm) as a carrier to insert two pairs of Teflon-coated fine-wire electrodes with a cross section of 76 μm (316-LVM-TF natural; California Fine-wire Company, USA) at 6 mm apart in the palpated muscle belly (Fig. 1A) through corresponding perforations in the HDsEMG grid. The carrier needle's direction was controlled using a special mechanical system mounted on a headset (Fig. 1B). The posterior fine-wire pair was inserted at maximum depth in the muscle, i.e. until the carrier needle tip touched the mandibular bone. The anterior fine-wire pair was positioned in the muscle tissue at a depth of only 3 mm, as determined by ultrasound scans prior to EMG data collections.

2.2.3. Scanning EMG

The two separate monopolar-needle EMG scans were performed using a monopolar scanning needle (Neuroline®, 38 × 0.36 mm, ø0.24 mm^2; Ambu GmbH, Bad Nauheim, Germany). For each scan, the needle was inserted into the electrode grid perforation at the center of one of the two previously inserted fine-wire pairs (Fig. 1A) and attached to a stepper motor. The motor was mounted on a head-supported mechanical system (Fig. 1B) to achieve a scanning direction parallel to the fine-wire insertion, and to ensure that movements made by the subject did not interfere with the measurement. Data were recorded during motor-driven scanning needle retraction in 50-μm steps at a fixed rate of three steps per second, beginning with the needle tip at the maximum depth. Needle retraction started once the subject reached the target force vector.

2.2.4. Bite force control

An intraoral 3D force transducer was mounted parallel to the mandibular occlusal plane on a metal splint (Schindler et al., 2005). Subjects were instructed to exert a constant, purely vertical bite force and to maintain this force vector throughout the scanning EMG procedure. Force magnitude was individually chosen based on the interference level in the fine-wire EMG so that the baseline was occasionally visible and, hence, decomposition of intramuscular EMG still appeared possible. Force values ranged between 15–40 N (average: 22 N).

2.2.5. Data acquisition

The HDsEMG was acquired in monopolar montage with a reference electrode attached behind the ear. The 256-channel amplifier (ActiveTwo; BioSemi, Amsterdam, The Netherlands) sampled at 4096 Hz with a resolution of 31.25 nV. The bipolar fine-wire EMG and monopolar scanning EMG were recorded with reference to a second surface electrode behind the right ear. These intramuscular signals were amplified, band-pass filtered (20 Hz–10 kHz), and digitized at a rate of 20 kHz (DantecKeypoint®; Natus Medical,

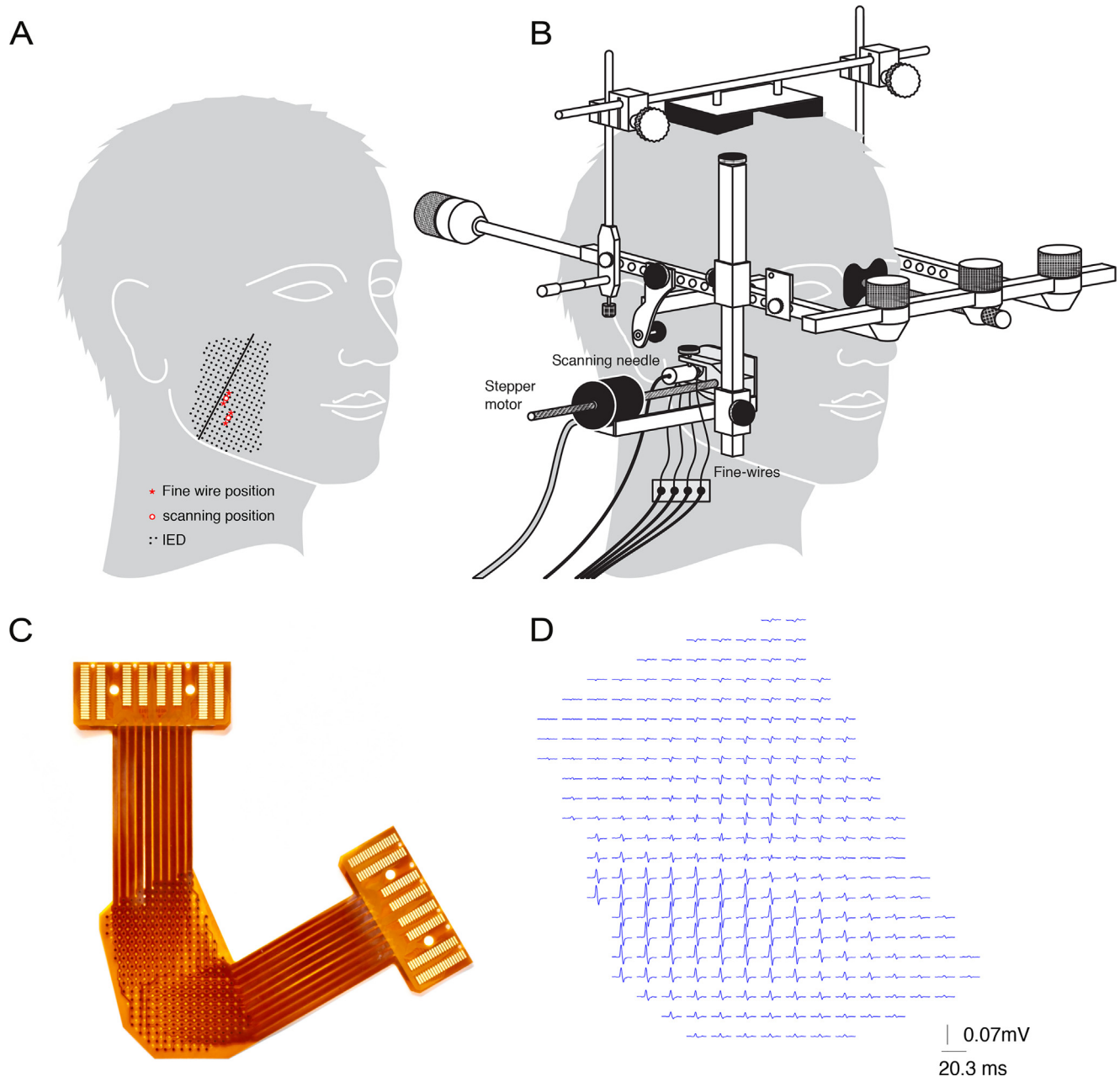

Fig. 1. A: Topographical representation of the EMG recordings using three different techniques: high-density surface electromyography (HDsEMG), intramuscular fine-wire EMG, and scanning EMG. Prior to attachment of the HDsEMG electrode grid, the region of the muscle belly was palpated and marked on the skin. A line was also drawn between the jaw angle and the lateral eye corner to standardize the electrode grid position across subjects. This line was centered between two specific electrode columns. Alignment of the electrode grid's lower border at the palpated lower mandibular border defined the vertical grid position. The two red circles mark the positions of the two separate EMG scans performed 10.8 mm apart in the region of the palpated muscle belly. Prior to each EMG scan, two bipolar fine-wire EMG electrodes (red stars) were inserted through perforations of the HDsEMG grid at a distance of 3 mm from the scanning EMG location in the cranial and caudal directions. This distance corresponds to the inter-electrode distance (IED) of the HDsEMG grid. B: Scheme of the measurement set-up, with the headset for guiding the fine-wire electrode insertions and for holding the stepper motor for retraction of the monopolar scanning needle. To provide a better overview, the surface EMG grid is not depicted in this panel. C: Photograph of the HDsEMG electrode grid comprising 256 regularly arranged, electrochemically deposited silver chloride electrode contacts with an inter-electrode distance (center-center) of 3 mm in both directions. The electrode grid was designed to cover the entire right masseter. D: Illustration of a decomposed MUAP showing the monopolar amplitude waveforms at each of the 256 single electrode locations (so-called MUAP template). (For interpretation of the references to colour in this figure legend, the reader is referred to the web version of this article.)

San Carlos, USA). The signal used to control the stepper motor was recorded via an opto-coupler and fed into both EMG amplifiers.

2.3. Data analysis

All data were analyzed in a Matlab programming environment (The Mathworks, Natick, USA).

2.3.1. Signal decomposition

The surface EMG signals were decomposed into MU action potentials (MUAPs, see examples in Figs. 1D, 2A and panel C of Supplementary Fig. S1) using the Convolution Kernel Compensation method (Holobar and Zazula, 2007). This decomposition technique has been validated for both synthetic and experimentally obtained HDsEMG signals from different muscles (Holobar et al., 2009; Holobar et al., 2010). After the automatic decomposition

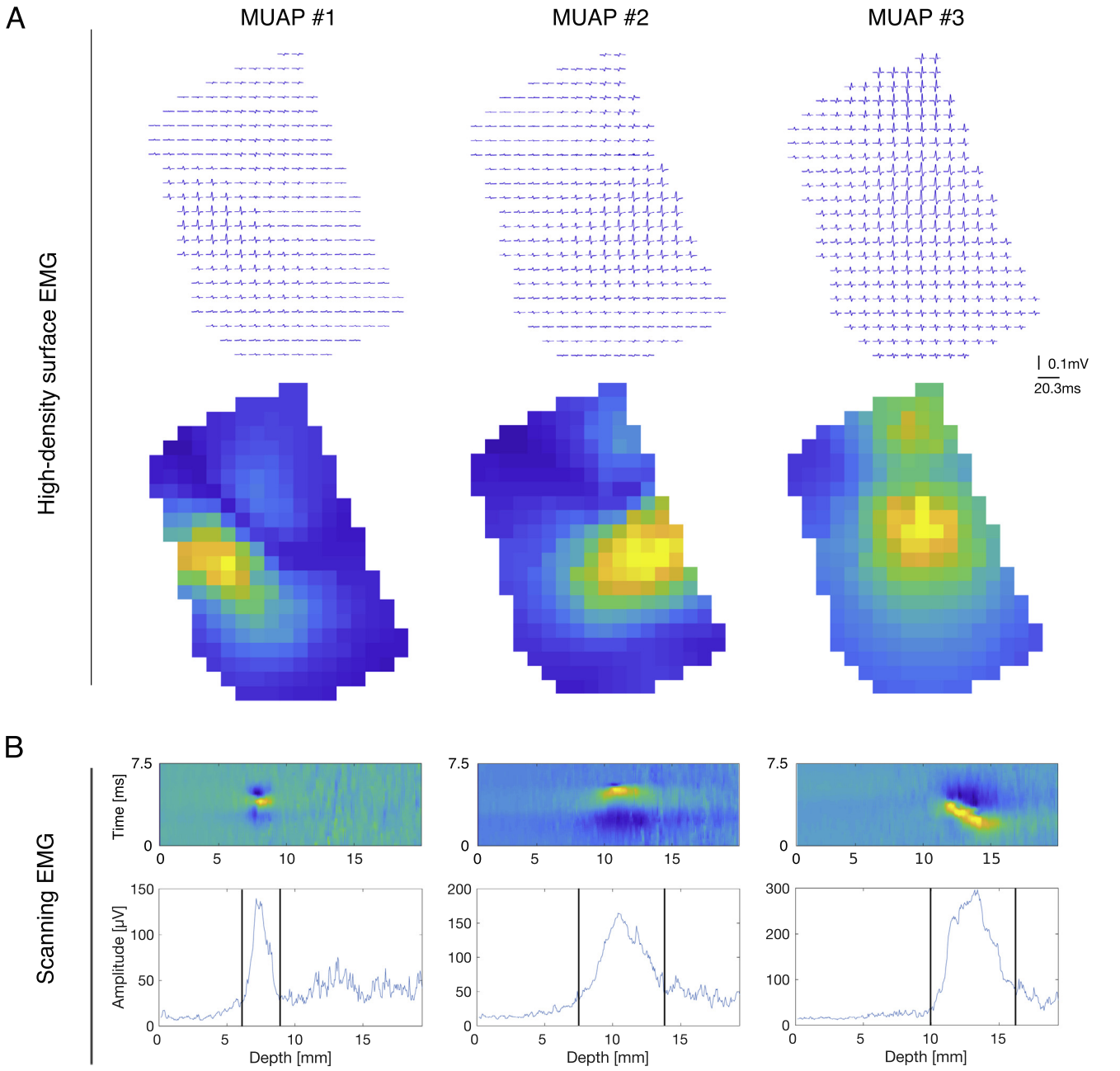

Fig. 2. A: Three examples of motor unit action potentials (MUAPs) decomposed from one high-density surface electromyography (HDsEMG) recording. The upper panels show the three MUAPs in the form of MUAP templates. The lower panels depict the same MUAPs as monopolar amplitude maps showing the color-coded root-mean-square (RMS) values of the MUAP waveforms at the 256 electrode locations. B: Amplitude profiles of the three MUAPs depicted in A) in the depth of the masseter. They were obtained by evaluation of the corresponding scanning EMG recordings. In both panels, the depth within the muscle (x-axis) is given as absolute values (in millimeters) measured from the skin surface as 0-mm reference. The upper panels show color-coded maps of the intramuscular MUAPs; the horizontal dimension of these color maps shows the amplitude of the MUAPs at different depths within the muscle; the vertical dimension of the color maps represents the time domain, i.e., the MUAP amplitude values at different latencies which corresponds to the amplitude waveform. The lower panels illustrate the maximum amplitudes of these MUAPs as a function of muscle depth. The medio-lateral diameters of the MUs are restricted by the deepest and the most superficial traces showing an amplitude clearly higher than noise level (pairs of black lines). (For interpretation of the references to colour in this figure legend, the reader is referred to the web version of this article.)

process, the validity of the results was evaluated based on the firing patterns obtained and the pulse-to-noise ratios (PNR) (Holobar et al., 2014). MUs with fewer than 10 firings and PNR values below 28 dB were discarded.

Fine-wire EMG data were decomposed using EMGlab (McGill et al., 2005). This program decomposes interference signals in a semi-automated way so that the user has full control over identification of each MU firing (see example for decomposition results in panel D of Supplementary Fig. S1).

2.3.2. Amplitude depth profiles of individual MUs

The amplitude profiles of decomposed MUs in the dimension of muscle depth were determined by spike-triggered averaging of the scanning needle signal using the firing patterns obtained by HDsEMG or fine-wire EMG, respectively. For each individual MU we then determined a 20-msec data window around each firing, reflecting the MU's action potentials in the scanning EMG signal. After band-pass filtering (10–5000 Hz), these intramuscular action potentials were averaged in each scanning step to obtain the mean

potential for that MU at that particular muscle depth. This procedure was performed for each needle retraction step, resulting in an individual scan for each decomposed MU (see examples in Fig. 2B). As a final step, a median filter was applied in the scanning direction to further reduce noise from non-time-locked activity (Gootzen et al., 1992). If the same MU was identified in both fine-wire signals and scanned twice, only one scan was saved. If no clear signal above noise level was present, we discarded the corresponding scan. More details about the scanning EMG procedure are given elsewhere (van Dijk et al., 2016).

2.3.3. MU parameters in the dimension of muscle depth

For each scanned MUAP we determined the positions of the deepest and the most superficial traces showing an amplitude clearly higher than noise level (Fig. 2B) to calculate the medio-lateral MU diameter (or territory, respectively) and the depth of the MU's center under the skin. These variables were averaged for individual subjects and for the pooled HDsEMG MUs or fine-wire MUs of all subjects. For individual subjects we also calculated the span of the medio-lateral MU diameters of all HDsEMG- or fine-wire-decomposed MUs to assess the portion of the muscle diameter from which MU activity was registered for each participant. All these positions and distances were also determined as relative values with reference to the individual medio-lateral masseter diameters. Local muscle and skin tissue thicknesses required for this normalization were estimated based on the scanning EMG raw signal characteristics.

2.3.4. Electrical MU size

Electrical MU size, which also reflects the anatomical MU size, was determined by averaging all the potentials in the scanning EMG belonging to the corresponding MU over a distance of 15 mm (resulting in a "virtual macro EMG signal" (van Dijk et al., 2016)), and by calculating the area under the resulting amplitude curve.

2.3.5. Two-dimensional projection of the MU's positions on the skin surface

In a HDsEMG MUAP, the electrode grid location with the largest negative monopolar peak amplitude corresponds to the location of the MU's endplate zone. This position can also be regarded as the MU's topographical position projected to the skin surface (Roeleveld et al., 1997; Lapatki et al., 2006).

The HDsEMG-decomposed MUAPs enabled direct determination of this variable. The surface representations (and subsequently the topographical positions) for all fine-wire-decomposed MUAPs were determined by spike-triggered averaging of the HDsEMG signals. Those triggered MUAPs showing no clear physiologic waveforms and amplitude distribution in the HDsEMG were discarded.

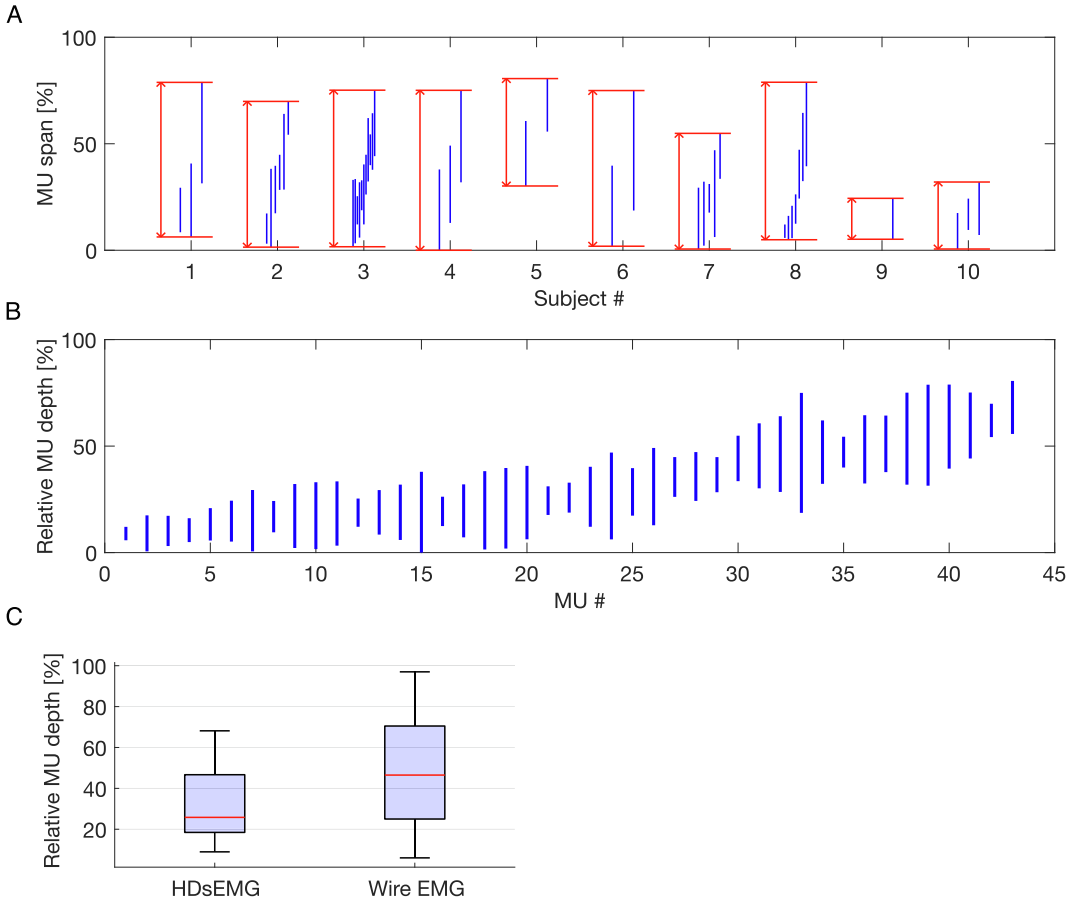

Fig. 3. A: Medio-lateral amplitude territories of the 43 motor units (MUs) that were decomposed from the high-density surface electromyography (HDsEMG) recordings and also visible in the scanning EMG. The blue bars represent the MUs' medio-lateral diameters within muscle depth. The latter variable is given as a percentage of the masseter's medio-lateral diameter at that location (0%: superficial masseter border, 100% deep masseter border). The MUs are sorted by subject; the red double arrows represent the medio-lateral span of all MUs identified in the corresponding subject. B: Pooled amplitude territories of the 43 HDsEMG-decomposed MUs (blue bars), sorted according to their relative depth within the masseter. C: Box plots illustrating the distribution of the medio-lateral territory centers of the 43 scanned HDsEMG-decomposed MUs (these centers reflect the middle of the blue bars depicted in B) compared to the territory centers of the 155 scanned fine-wire decomposed MUs. (For interpretation of the references to colour in this figure legend, the reader is referred to the web version of this article.)

Table 1
Descriptive statistics for the MUs decomposed from the high-density surface electromyography (HDsEMG) recordings, and the fine-wire EMG recordings.

	Scanned HDsEMG MUs (N = 43)					Scanned fine-wire EMG MUs (N = 155)				
	Min.	1. Q.	Med.	3. Q.	Max.	Min.	1. Q.	Med.	3. Q.	Max.
Pooled MUs of all subjects										
Depth of MU center from skin (mm) †	4,1	8,7	9,9	12,2	17,7	4,3	9,8	12,2	16,8	24,4
Depth of MU center within muscle (%) ‡	8,9	18,6	25,8	46,5	68,2	8,5	25,8	47,1	70,8	96,6
Medio-lateral MU diameter (mm)	1,2	2,6	4,4	5,0	7,9	0,6	2,7	3,9	4,8	8,6
Electrical MU size (μVms)	15.7	116.5	172.3	375.1	789.8	15.9	119.7	186.7	338.7	1100.4
MU samples of individual subjects										
Decomposed MUs §	8	11	15,5	26,75	40	11	28,5	33,5	35,5	47
Scanned MUs	1	2,25	3	5,75	11	6	8,75	15	21,25	29
Medio-lateral span of MUs (mm)	3,3	7,5	9,2	14,1	16,5	7,7	12,9	15,7	17,6	20,5
Medio-lateral span of MUs (%) ‡	19,2	51,4	70,5	73,4	75,1	71,6	87,2	94,8	97,0	99,3
Lateral border of MU span (mm) †	2,3	3,8	6,0	6,5	7,9	2,4	3,6	5,4	6,4	7,7
Lateral border of MU span (%) ‡	0,0	0,8	1,8	5,1	30,2	0,0	1,0	1,8	4,7	8,5
Medial border of MU span (mm) †	11,1	14,3	15,3	18,0	19,0	14,9	18,2	21,2	22,7	25,0
Medial border of MU span (%) ‡	24,4	58,6	75,0	77,9	80,6	77,2	92,1	97,4	99,6	100

† absolute distances to the skin surface in millimeters.
‡ relative depth within the masseter as a percentage; 0%: superficial masseter border, 100%: deep masseter border.
§ total number of HDsEMG-decomposed MUs: 190; total number of fine-wire EMG-decomposed MUs: 271.

2.4. Statistical analysis

Differences between the HDsEMG- and fine-wire-EMG MU samples were analyzed using the Mann-Whitney-U-test; for the paired variables calculated for individual subjects we used the Wilcoxon-signed-rank-test. The *p*-values were adjusted for multiple testing using the Hochberg method.

3. Results

A total of 190 MUs were decomposed from the HDsEMG data recorded during the two EMG scans. The average number of firings identified per MU was 1799 (range: 156–3786). Forty-three (23%) of these MUs showed an action potential in the scanning EMG. From the 271 MUs decomposed from the fine-wire signals, 155 (58%) showed a visible action potential in the scanning EMG.

Results for the HDsEMG-decomposed MUs and fine-wire-decomposed MUs are compared in Fig. 3 and Table 1 (results for fine-wire MUs have already been partially reported previously (van Dijk et al., 2016)). Median depth of the centers of the pooled HDsEMG-decomposed MUs was 9.9 mm under the skin surface, corresponding to a relative depth of 25.8% within the masseter's medio-lateral diameter (Fig. 3C). In comparison, the fine-wire-decomposed MUs were located significantly deeper (Mann-Whitney-U test, adjusted $p = 0.002$), with a median depth of 12.2 mm corresponding to 47.1% of muscle depth.

The median medio-lateral diameter of 4.4 mm of the pooled HDsEMG-decomposed MUs did not differ significantly (Mann-Whitney-U test, adjusted $p = 0.805$) from that of the fine-wire-decomposed MUs (3.9 mm). Also the other evaluated variable describing the size of a MU, i.e. electrical MU size, showed no significant difference between the HDsEMG-decomposed MUs and fine-wire-decomposed MUs (Mann-Whitney-U test, adjusted $p = 0.812$), with median values of 172.3 μVms and 186.7 μVms, respectively. This variable showed a skewed distribution towards smaller values in both MU samples.

The medio-lateral diameters of the HDsEMG-decomposed MUs and their position depths showed a weak positive correlation (Spearman's rank correlation coefficient $r = 0.257$, $p = 0.048$ for one-sided test of positive correlation), while there was no signifi-

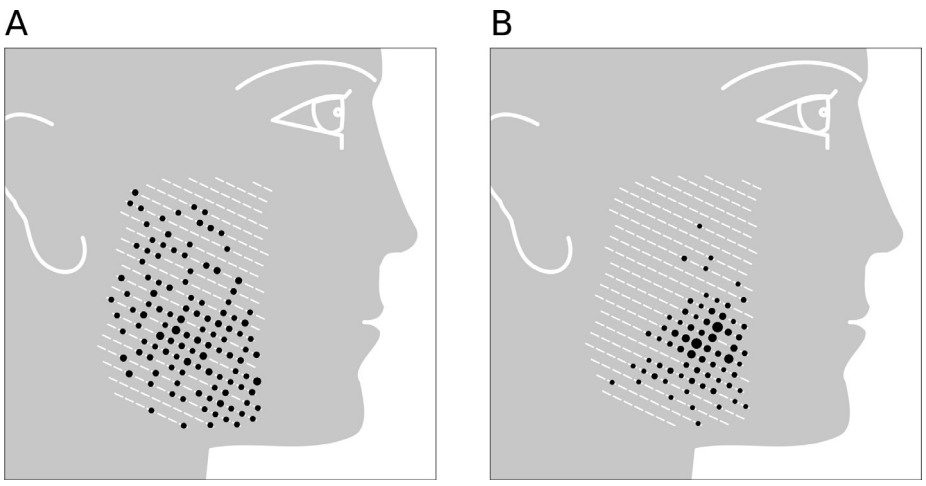

Fig. 4. A: Topographical distribution of the 190 motor units (MUs) decomposed from the high-density surface electromyography (HDsEMG) recordings. The different diameters of the black dots represent the numbers of MUs localized at a specific electrode location. For the HDsEMG-decomposed MUs this number ranged between 1–6 MUs. B: Topographical distribution of the fine-wire-decomposed MUs; of the 271 decomposed MUs, 208 showed a visible action potential on the HDsEMG grid. According to the diameters of the black dots, the numbers of MUs localized at the different electrode locations ranged between 1–15 MUs.

cant correlation found between these variables for the fine-wire-decomposed MUs ($r < -0.001$, $p = 0.502$). Although deeper HDsEMG-decomposed MUs slightly tend to have a larger medio-lateral diameter, Fig. 3B illustrates that the HDsEMG technique recorded MUs with larger or smaller medio-lateral diameters both deeper and more superficially within the muscle.

For individual subjects, the medio-lateral diameters of the HDsEMG-decomposed MUs spanned 70.5% of the masseter's diameter (Fig. 3A). For comparison, the fine-wire-decomposed MUs spread into a significantly greater muscle diameter (Wilcoxon-signed-rank test, $p = 0.016$), with a median value of 94.8%. For individual subjects, the spread of the HDsEMG- and fine-wire-decomposed MUs into the superficial masseter portion was quite similar; HDsEMG-decomposed MUs, however, reached a relative median depth of only 75.0%, whereas fine-wire-decomposed MUs extended to statistically deeper masseter portions (Wilcoxon-signed-rank test, $p = 0.016$), with a median depth of 97.4% (Table 1).

Fig. 4 shows the MUs' topographical positions projected to the skin surface for all HDsEMG- or fine-wire-decomposed MUs. Obviously, the 190 HDsEMG-decomposed MUs are more or less widely distributed over the entire masseter (Fig. 4A), whereas most of the 208 fine-wire-decomposed MUs showing an action potential in the HDsEMG above the noise level are concentrated in approximately ¼-th of the muscle's surface around the fine-wire locations (Fig. 4B).

4. Discussion

By using high-density sEMG and advanced signal processing software it has been possible to study individual MUs of the masseter muscle with a non-invasive approach. Because this method enables evaluation of both recruitment and firing behavior, and of surface-topographical characteristics of individual MUs, it might indeed be an ideal tool for refined pathophysiological and clinical studies of TMD patients.

Any method obtaining information about individual MUs only takes a sample from the entire MU pool of the muscle investigated. Considering the possible future application of HDsEMG for diagnostic purposes, an important question is the extent to which the extracted MU sample represents activity of the entire masseter. This particularly applies to a complex muscle such as the masseter, which has distinguishable anatomical muscle compartments and shows differential activation (Widmer et al., 2003; Cioffi et al., 2012). This study addressed this issue by combining HDsEMG with scanning EMG to characterize the MUs' amplitude topographies three-dimensionally. Such an approach is, to the best of our knowledge, novel for any skeletal muscle. Our results revealed that MUs detected by HDsEMG spanned on average 70.5% of the masseter's diameter in individual subjects, which means that this non-invasive technique detects MU activity from the predominant masseter portion. The median medio-lateral diameters of the HDsEMG-decomposed MUs (4.4 mm) and the fine-wire-decomposed MUs (3.9 mm) are in good agreement with the scanned mean MU diameters of 3.7 mm reported in two previous studies (Stålberg and Eriksson, 1987; Tonndorf and Hannam, 1994). Although in the current study the difference between median MU diameters of HDsEMG-decomposed and fine-wire-decomposed MUs was not statistically significant, it might be speculated that the slight tendency of HDsEMG-decomposed MUs towards a larger median diameter might be due to certain limitations of the HDsEMG technique in detecting very small MUs in the deepest regions of the muscle.

Based on the relatively small number of scanned HDsEMG MUs per subject and the fact that MUs were certainly not always scanned at their largest diameter, we speculate that a complete decomposed HDsEMG MU sample of an individual actually spans an even wider proportion of the masseter's cross-section. Evaluation of EMG scans showed that in particular smaller MUs with an amplitude territory in the deepest masseter portion (i.e., the 25% located near the mandibular bone, Table 1) were less accessible for HDsEMG. This means that in the dimension of muscle depth, the representativeness of a HDsEMG-decomposed MU sample would only be compromised if the very deep MUs are involved in different functional tasks from the more superficial MUs. However, such subdivision of the human masseter into larger functional compartments seems to be contradicted by previous studies which showed that during different motor tasks, the relationship between activity in the deep and superficial masseter portions is relatively stable, and that MU task grouping seems to occur in quite small subvolumes instead of larger muscle compartments (Schindler et al., 2014; Terebesi et al., 2015).

Regarding the other two spatial dimensions, i.e. those parallel to the muscle's outer surface, our results revealed that MU samples detected by fine-wire EMG are topographically restricted to approximately one fourth of the masseter's surface. In contrast, HDsEMG is able to detect active MUs that are distributed over the entire muscle and provides their complete amplitude surface profiles. This seems ideal for answering important clinical questions such as how to identify the causes of painful muscles, or effects of therapeutic interventions. Moreover, providing a window on the motoneuron level to study the reorganization of MU task groups while keeping a broader topographical view of the entire muscle may be an essential advantage in clinical applications (Zwarts and Stegeman, 2003).

In the discussion regarding which technique is preferable for MU studies of TMD patients, not only the representativeness of a detected MU sample, but also measurement reproducibility and patient concerns have to be considered. An important limitation of intramuscular EMG is the impossibility of repositioning a needle or fine-wire electrode for follow-up measurements at the specific location used for previous recordings. Hence, reproducibility in repeated measurements—which is essential for long term monitoring—would be far lower if using an intramuscular EMG technique instead of HDsEMG recordings from the entire muscle (Rainoldi et al., 1999; Maathuis et al., 2008). Particularly for patients with muscle pain, the non-invasiveness of HDsEMG is another indisputable and important advantage.

Both decomposition of intramuscular fine-wire EMG and HDsEMG is limited with regard to the force level up to which signals are decomposable. In this study, the force levels examined were adjusted to the maximum decomposable amplitude level of the fine-wire EMG signals to obtain a comparable MU sample as "gold standard". The target force levels applied corresponded to approximately 20% of maximal voluntary contraction. For the masseter it is known that at a level of 10–20% of maximal voluntary contraction, approximately 50% of all MUs are already recruited (Derfler and Goldberg, 1978). Follow-up experiments are to be carried out to explore the maximum bite force up to which a sample of individual MUs can be extracted from the masseter using HDsEMG. Based on the results of corresponding studies for other muscles (Holobar et al., 2010, 2014) it can be hypothesized that decomposable force is also higher in the masseter when HDsEMG is used instead of intramuscular fine-wire EMG.

5. Conclusions

HDsEMG recordings from the masseter can be decomposed into the contributions of individual MUs, which makes it possible to study their recruitment and firing behavior non-invasively. Com-

pared to full decomposition of intramuscular fine-wire or needle EMG signals, evaluation of HDsEMG data is relatively time efficient because it requires less user interaction. This surface-EMG-based technique seems somewhat limited in capturing very small MUs located in the deepest 25% of the masseter's cross-section. This seems less problematic, however, because even for low contraction levels, MUs with different sizes are active throughout the entire muscle cross-section. Whereas intramuscular techniques record MU activity in a restricted muscle region, HDsEMG is the only method that detects MUs from the entire muscle surface. From a three-dimensional point of view, this non-invasive method may therefore be considered more representative and reproducible than intramuscular EMG. Overall, we conclude that HDsEMG is a promising non-invasive tool for studying the control of painful muscles and monitoring long-term neuromuscular reorganization as may occur for TMD patients treated by various therapeutic interventions. Future research involving controlled experimental pain in healthy subjects may be a first step toward application of this electrophysiological technique for TMD patients.

Acknowledgements

The statistical analysis was supported by Stefan Repky (Institute of Statistics, University of Ulm, Germany). Development of the applied decomposition method was supported by the Slovenian Research Agency, Slovenia (grant numbers J2-7357 and P2-0041).

Disclosures

We confirm that none of the authors have potential conflicts of interest associated with this publication to be disclosed, and that there has been no significant financial support for this work that could have influenced its outcome.

Appendix A. Supplementary material

Supplementary data associated with this article can be found, in the online version, at https://doi.org/10.1016/j.clinph.2018.12.008.

References

Blok JH, Van Dijk JP, Drost G, Zwarts MJ, Stegeman DF. A high-density multichannel surface electromyography system for the characterization of single motor units. Rev Sci Instrum 2002;73:1887–97.
Cioffi I, Gallo LM, Palla S, Erni S, Farella M. Macroscopic analysis of human masseter compartments assessed by magnetic resonance imaging. Cells Tissues Organs 2012;195:465–72.
Derfler B, Goldberg LJ. Spike train characteristics of single motor units in the human masseter muscle. Exp Neurol 1978;61:592–608.
van Dijk JP, Eiglsperger U, Hellmann D, Giannakopoulos NN, McGill KC, Schindler HJ, et al. Motor unit activity within the depth of the masseter characterized by an adapted scanning EMG technique. Clin Neurophysiol 2016;127:3198–204.
Dworkin SF, LeResche L. Research diagnostic criteria for temporomandibular disorders: review, criteria, examinations and specifications, critique. J Craniomandib Disord 1992;6:301–55.
Falla D, Farina D, Graven-Nielsen T. Experimental muscle pain results in reorganization of coordination among trapezius muscle subdivisions during repetitive shoulder flexion. Exp Brain Res 2007;178:385–93.
Falla D, Lindstrøm R, Rechter L, Farina D. Effect of pain on the modulation in discharge rate of sternocleidomastoid motor units with force direction. Clin Neurophysiol 2010;121:744–53.
Gootzen TH, Vingerhoets DJ, Stegeman DF. A study of motor unit structure by means of scanning EMG. Muscle Nerve 1992;15:349–57.
Holobar A, Farina D, Gazzoni M, Merletti R, Zazula D. Estimating motor unit discharge patterns from high-density surface electromyogram. Clin Neurophysiol 2009;120:551–62.
Holobar A, Minetto M, Farina D. Accurate identification of motor unit discharge patterns from high-density surface EMG and validation with a novel signal-based performance metric. J Neural Eng 2014;11:016008.
Holobar A, Minetto MA, Botter A, Negro F, Farina D. Experimental analysis of accuracy in the identification of motor unit spike trains from high-density surface EMG. IEEE Trans Neural Syst Rehabil Eng 2010;18:221–9.
Holobar A, Zazula D. Multichannel blind source separation using convolution Kernel compensation. IEEE Trans Signal Process 2007;55:4487–96.
Lapatki BG, Van Dijk JP, Jonas IE, Zwarts MJ, Stegeman DF. A thin, flexible multielectrode grid for high-density surface EMG. J Appl Physiol 2004;96:327–36.
Lapatki BG, Oostenveld R, Van Dijk JP, Jonas IE, Zwarts MJ, Stegeman DF. Topographical characteristics of motor units of the lower facial musculature revealed by means of high-density surface EMG. J Neurophysiol 2006;95:342–54.
List T, Dworkin SF. Comparing TMD diagnoses and clinical findings at Swedish and US TMD centers using research diagnostic criteria for temporomandibular disorders. J Orofac Pain 1996;10:240–53.
Maathuis EM, Drenthen J, Dijk JP Van, Visser GH, Blok JH. Motor unit tracking with high-density surface EMG. J Electromyogr Kinesiol 2008;18:920–30.
Manfredini D, Guarda-Nardini L, Winocur E, Piccotti F, Ahlberg J, Lobbezoo F. Research diagnostic criteria for temporomandibular disorders: a systematic review of axis i epidemiologic findings. Oral Surg Oral Med Oral Pathol Oral Radiol Endod 2011;112:453–62.
McGill KC, Lateva ZC, Marateb HR. EMGLAB: an interactive EMG decomposition program. J Neurosci Methods 2005;149:121–33.
Merletti R, Botter A, Troiano A, Merlo E, Minetto MA, Alessandro M. Technology and instrumentation for detection and conditioning of the surface electromyographic signal: state of the art. Clin Biomech 2009;24:122–34.
Minami I, Akhter R, Albersen I, Burger C, Whittle T, Lobbezoo F, et al. Masseter motor unit recruitment is altered in experimental jaw muscle pain. J Dent Res 2013;92:143–8.
Rainoldi A, Galardi G, Maderna L, Comi G, Lo Conte L, Merletti R. Repeatability of surface EMG variables during voluntary isometric contractions of the biceps brachii muscle. J Electromyogr Kinesiol 1999;9:105–19.
Roeleveld K, Stegeman DF, Falck B, Stålberg EV. Motor unit size estimation: confrontation of surface EMG with macro EMG. Electroencephalogr Clin Neurophysiol 1997;105:181–8.
Schindler HJ, Hellmann D, Giannakopoulos NN, Eiglsperger U, van Dijk JP, Lapatki BG. Localised task-dependent motor-unit recruitment in the masseter. J Oral Rehabil 2014;41:477–85.
Schindler HJ, Rues S, Türp JC, Schweizerhof K, Lenz J. Activity patterns of the masticatory muscles during feedback-controlled simulated clenching activities. Eur J Oral Sci 2005;113:469–78.
Stålberg E, Eriksson PO. A scanning electromyographic study of the topography of human masseter single motor units. Arch Oral Biol 1987;32:793–7.
Terebesi S, Giannakopoulos NN, Brüstle F, Hellmann D, Türp JC, Schindler HJ. Small vertical changes in jaw relation affect motor unit recruitment in the masseter. J Oral Rehabil 2015;43:259–68.
Tonndorf ML, Hannam AG. Motor unit territory in relation to tendons in the human masseter muscle. Muscle Nerve 1994;17:436–43.
Türp JC, Schindler HJ, Pritsch M, Rong Q. Antero-posterior activity changes in the superficial masseter muscle after exposure to experimental pain. Eur J Oral Sci 2002;110:83–91.
Widmer CG, Carrasco DI, English aW. Differential activation of neuromuscular compartments in the rabbit masseter muscle during different oral behaviors. Exp Brain Res 2003;150:297–307.
Zwarts MJ, Stegeman DF. Multichannel surface EMG: basic aspects and clinical utility. Muscle Nerve 2003;28:1–17.